Sleep, 18(7):557–564

Sleep EEG and Snoring

Age and Gender Affect Different Characteristics of Slow Waves in the Sleep EEG

M. S. Mourtazaev, B. Kemp, *A. H. Zwinderman and H. A. C. Kamphuisen

Department of Neurology and Clinical Neurophysiology of Leiden University Hospital; and
**Department of Medical Statistics of Leiden State University, The Netherlands*

Summary: Low-frequency EEG was analyzed quantitatively during 2 nights in 40 females and 34 males aged 26 to 101 years. Analyses were based on Rechtschaffen and Kales NREM sleep stages, on absolute low-frequency amplitude (i.e. power in the range of 0.2–2.0 Hz) and on low-frequency continuity. The latter parameter describes how much (0–100%) of the current slow-wave activity is continued in the near-future EEG. Such continuation can occur through closed loops in the underlying neuronal network and cells. These loops are slow, thus corresponding to slow-wave frequencies, and can consist of electrophysiological, chemical and/or other pathways. The continuity percentage then monitors the relative activity of these loops. It does not depend directly on absolute EEG amplitudes.

All analyzed parameters, including amplitude-independent continuity, decreased substantially and significantly with increasing age. The amplitudes of low-frequency EEG in females were significantly and substantially (40%) larger than those in males. However, the amplitude-independent continuity percentage did not differ between the genders.

These findings support the notion that gender-related anatomical differences have a general effect on EEG amplitude, including during slow-wave sleep. Aging, however, specifically affects the neurophysiological slow-wave-generating mechanism. **Key Words:** Age—Gender—Sleep—Electroencephalography.

Standard visual discrimination (1) of NREM sleep stages is largely based on slow-wave activity in the EEG. Although the relationship between slow-wave EEG activity and NREM sleep seems to be rather firm (2–4), the amplitude and percentage thresholds involved in distinguishing stages 2, 3 and 4 bias the results.

Computer analysis of NREM sleep is usually based on quantification of the low-frequency power and/or amplitude, e.g. using Fourier analysis, without involving any threshold. The result is an estimate of NREM slow-wave intensity on a continuous intensity scale (5,6).

Such computer analysis and visual scoring of NREM sleep both depend strongly on the amplitude of the slow waves. This amplitude-dependence is a potential shortcoming in the following two cases.

First, if slow-wave amplitudes were to vary while the physiological NREM sleep depth remained constant, then this variation would introduce bias or at least inaccuracy in amplitude-based sleep analysis. The possibility that slow-wave amplitudes vary within a given NREM sleep stage is one of the arguments for smoothing within epochs in manual sleep scoring. The variability can also be seen in neuronal network models that have simulated EEG with strongly waxing and waning rhythms and slow waves even when these models had constant parameters (7,8). Therefore, although experimental evidence is lacking, we must consider the possibility that slow-wave amplitudes vary even when physiological sleep depth does not.

Second, if low-frequency EEG amplitudes differ between subjects for reasons unrelated to NREM sleep depth, then amplitude-based sleep analysis will be biased. Many factors unrelated to NREM sleep depth, including brain anatomic orientation, thickness of the skull, gender and headsize, are known to influence the low-frequency EEG amplitudes. These factors do vary considerably between subjects.

Zero-cross slow-wave analysis (9,10) is less amplitude-dependent. However, especially at low amplitudes, other EEG components can dominate the analysis. Moreover, the method does not utilize additional information in the signal between zero-crossings. As a consequence, the basic intensity/time resolution is limited to a yes/no decision about (in this case) every 1

Accepted for publication May 1995.
Address correspondence and reprint requests to Dr. B. Kemp, University Hospital Leiden, Department of Neurology and Clinical Neurophysiology, P.O. Box 9600, NL-2300 RC Leiden, The Netherlands.

second. This gives relatively limited possibilities for variance reduction.

An amplitude-independent analysis method (11,12; see also the Appendix) has been developed that has a physiological background (7,8,13–16), utilizes the whole signal and basically produces a continuous intensity value every 0.01 second.

The physiological background of this analyzer is the assumption of closed loops in the slow-wave-generating neuronal network and cells. These loops are slow, thus corresponding to slow-wave frequencies, and can consist of electrophysiological, chemical and/or other pathways. The loops can continuously pass current slow-wave activity to the future EEG, thus making the system resonate. With increasing NREM sleep depth, an increasing percentage of these potentially resonating loops is activated and actually resonating, resulting in increasing slow-wave intensity. Models of such networks simulate EEG with strongly waxing and waning rhythms and slow waves, even when the percentage of activated loops is constant (7,8). Apparently, an implicit assumption of the model is that short-term variations in amplitude do not necessarily reflect changes in sleep depth.

The model-based analyzer estimates the active percentage (0–100%) of potentially resonating loops. It does this simply by continuously monitoring how much (0–100%) of the current slow-wave component is actually continued in the near-future EEG. The analysis result, i.e. the continuity percentage, does not depend on absolute EEG amplitudes, calibration or amplifier settings. It remains constant during simulated waxing and waning slow-wave bursts. The analyzer has already proven its practical value in other applications (17–20).

In this study we aimed to establish how age and gender affect NREM sleep EEG, and in particular whether the neuronal slow-wave-generating mechanism itself is involved. For this purpose we analyzed age and gender effects on NREM sleep in 74 subjects based on Rechtschaffen and Kales NREM sleep stages, on absolute slow-wave amplitudes (i.e. power) and on the amplitude-independent slow-wave continuity.

MATERIALS AND METHODS

The data of ambulatory polysomnograms of 74 subjects from 26 to 101 years of age recorded in an earlier study (21) were used for this study.

Subjects were recruited from the local population in the period 1989–1991. All subjects had a half-hour interview and another half-hour medical/neurological examination by a neurologist/psychiatrist (H.A.C.K.). They showed no somatic, neurologic or psychiatric disorders; however, some persons from the "senior" age group were found to have moderate visual and/or hearing loss. Subjects had neither sleep complaints nor did they use sleep-related medication. The subjects were grouped by age and gender (F: females, M: males) as follows: 26–35 years (10 F, 9 M), 51–60 years (12 F, 8 M), 66–75 years (10 F, 9 M) and 85–101 years (8 F, 8 M). During the recording period, subjects were instructed to maintain their habitual activity patterns and not to use any drugs. Most young volunteers were instructed and underwent the electrode placement procedure at the hospital. Subjects from the "senior" age group underwent this procedure at their residences, performed by a visiting physician accompanied by an EEG technician.

For each subject a 48-hour ambulatory polysomnogram was recorded at home using a modified Oxford four-channel cassette recorder (11) with frequency response range (3 dB points) from 0.5 to 100 Hz. Electrode resistances were <5 kOhm at the start of the recording. The recorded signals were EEG (FpzCz and PzOz), horizontal EOG, submental EMG, event marker and crystal-clocked time. The records were digitized (12 bits/sample) in a personal computer (PC), with the 100-Hz sampling frequency being continuously synchronized to the recorded time signal. Digital amplitudes were standardized using amplitude calibration signals which had also been recorded. Noise levels were checked using zero-voltage calibration signals that were also recorded. Adequate maintenance of the recorder was guaranteed because recordings were automatically deleted if the full-bandwidth (0.5–100 Hz) noise level of an EEG channel exceeded 7 μV rms. Only the nights, i.e. both 10-hour periods starting at "lights-off", were analyzed.

Both visual and automatic analyses of slow-wave activity were performed on PCs. All recordings were analyzed according to the following procedure.

First, Rechtschaffen and Kales (R&K) sleep stages were manually scored (PC-aided) in 30-second epochs according to standard criteria (1).

The analyzer automatically rejected 1-second epochs in which the EEG was unlikely to have originated from the modeled neuronal resonance mechanism. The artifact rejection algorithm is described in the Appendix. Constant low and high thresholds were empirically tuned (in an earlier study) in such a way that most periods with clear mains interference, EMG artifact, low-frequency EOG or body movements were rejected.

The slow-wave power (SWP) of the EEG was computer-estimated in the remaining epochs based on the bandpass filter (0.5–2.0 Hz) described by Kemp and Lopes da Silva (12). The slow-wave continuity percentage (SW%) was computed in the same frequency band using the algorithms also described by Kemp and Lopes da Silva (12). Smoothing was applied, as was

interpolation over artifact-rejected epochs. The result was a whole-night automatically computed continuous SWP and SW% plot (see Fig. 1).

In order to avoid introducing bias due to artifacts that had not been rejected by the purely automatic procedure described above, the continuous SWP and SW% plots were also computed after additional tedious manual artifact rejection at a PC by an experienced neurophysiologist (M.S.M.). He took 15 of the 74 subjects out of the data set because one or both nights of their recording had a continuous period of 5 minutes or more with loss of signal (e.g. caused by loosely connected electrodes) and/or technical artifacts (e.g. mains interference) and/or heartbeat artifacts. In the remaining 59 subjects (see Table 1), he rejected all 1-second epochs that had clear artifacts. These manually rejected artifacts arose mainly from body or eye movements, respiration and, probably, excessive sweating.

This procedure thus resulted for each recorded period in five "plots": a manual R&K hypnogram, one automatic and one "manual" SWP plot and one automatic and one "manual" SW% plot. A typical example is shown in Fig. 1.

From each of these five plots we derived the following parameters that characterize NREM sleep:

- SWS duration: the amount of time spent in SWS.
- NREM total: NREM area (time by intensity).
- NREM maximum: the deepest NREM sleep reached.

The exact definitions of the R&K-derived parameters are:

- SWS duration (minutes): time spent in stage 3 or 4.
- NREM total (stage·minutes): area exceeding stage 1.
- NREM maximum: deepest NREM stage.

The exact definitions of the "manual" and automatic SWP-derived parameters are:

- SWS duration (minutes): time with SWP > 300 μV^2.
- NREM total (μV^2·minutes): SWP area exceeding 200 μV^2.
- NREM maximum (μV^2): maximum value of SWP.

The exact definitions of the "manual" and automatic SW%-derived parameters are:

- SWS duration (minutes): time with SW% > 70%.
- NREM total (%·minutes): SW% area exceeding 50%.
- NREM maximum (%): maximum value of SW%.

The 300-μV^2 and 200-μV^2 thresholds in the definitions of the SWP-derived duration and total were chosen because they best select (although still not very well) R&K-defined SWS and NREM periods, respectively. The 70% and 50% thresholds in the definitions of the SW%-derived duration and total were chosen for the same reason. In this way, differences between R&K-, SWP- and SW%-based results are less likely to result from having analyzed different periods of the sleep process.

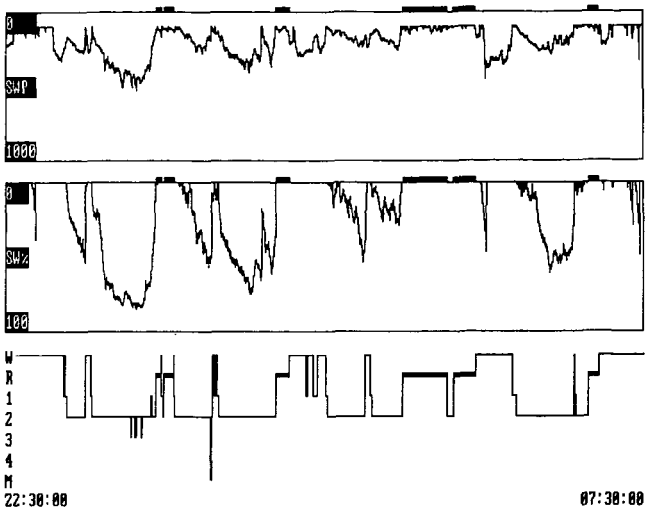

FIG. 1. A 9-hour sleep–wake recording (4,201/89). From top to bottom: slow-wave power (SWP, in μV^2), slow-wave continuity (SW%), hypnogram (R&K). Note that all traces reflect the ultradian rhythm. This female, aged 56, had relatively low amplitudes, as reflected by the SWP trace and the hypnogram, but still relatively high slow-wave continuity, as reflected by the SW% trace. Note also that SWP is more sensitive to artifacts during some of the wakefulness periods than SW%. No manual artifact rejection was applied.

The thresholds also automatically reject most of the undetectable low-amplitude artifacts that might remain after the rejection procedures described above. Of course, the maximum parameters do not involve any threshold.

The thresholds were formally derived by R.O.C. analysis. They optimally detected R&K-defined SWS and NREM periods, respectively, from the manually influenced SWP and SW% plots of the youngest age category.

The above-defined nine parameters were computed for each 48-hour recording as well as for each 24-hour half of it. The computations were carried out for both the manually influenced and purely automatic plots.

The "automatic" data set thus consisted of the following parameters for each of 74 subjects: the nine first-night parameters, the nine second-night parameters and the nine both-nights parameters. The "manual" data set consisted of the same parameters for each of 59 subjects.

Statistical analysis

These data sets were analyzed with SPSS® for Windows (SPSS Inc. 1993). We considered p values of <0.05 statistically significant. Age and gender effects

TABLE 1. *Quantity of NREM sleep in the both-nights data set after manual artifact rejection; 59 subjects grouped by age and gender*

Age	26–35 years		51–60 years		66–75 years		85–101 years	
Gender	F (10)	M (8)	F (8)	M (6)	F (9)	M (6)	F (5)	M (7)
Duration	154	137	66	30	117	28	80	10
R&K	(78)	(71)	(58)	(60)	(87)	(20)	(98)	(16)
Duration	337	167	142	17	222	2	143	28
SWP	(146)	(78)	(154)	(31)	(82)	(2)	(256)	(71)
Duration	198	232	117	100	101	105	138	73
SW%	(110)	(102)	(28)	(47)	(77)	(96)	(132)	(75)
Total	829	754	594	543	671	511	633	417
R&K	(152)	(126)	(147)	(110)	(178)	(96)	(153)	(62)
Total	187,088	61,125	44,727	4,798	67,334	1,768	34,948	5,939
SWP	(113,523)	(33,895)	(58,791)	(8,521)	(27,260)	(1,724)	(60,960)	(15,073)
Total	8,308	9,823	4,785	4,242	4,425	4,593	6,125	3,827
SW%	(4,968)	(4,459)	(1,064)	(1,787)	(2,676)	(3,355)	(4,884)	(2,912)
Maximum	4.00	3.87	3.50	3.00	3.89	3.50	3.20	2.71
R&K	(0.00)	(0.35)	(0.53)	(0.89)	(0.33)	(0.55)	(0.84)	(0.76)
Maximum	1,915	907	612	274	709	289	430	248
SWP	(900)	(289)	(277)	(144)	(205)	(75)	(200)	(198)
Maximum	92.9	93.6	88.1	85.5	84.3	83.3	85.4	80.9
SW%	(3.6)	(3.9)	(2.6)	(6.0)	(6.4)	(8.0)	(5.4)	(5.7)

From top to bottom all nine NREM parameters: the three basic NREM sleep parameters Duration, Total, and Maximum, each computed from 48-hour NREM plots based on R&K stages (R&K), slow-wave power (SWP), and slow-wave continuity (SW%), respectively. Each of the four age groups is subdivided by gender, F and M, with the number of subjects in parentheses. For each subgroup and each parameter, the table lists the within-group mean and SD (in parentheses).

were assessed by a two-way (age by gender) analysis of variance (ANOVA). Significantly interacting age and gender effects were also assessed by one-way ANOVA within gender and age groups. Age groups were also compared pairwise using the Student-Newman-Keuls test. Differences between the first and second nights were evaluated using a paired t test.

RESULTS

First-night effect

No significant difference between the first and second nights was observed for any of the nine NREM sleep parameters obtained from either the automatic or the manual data set. The 18 p values ranged (over the parameters) from 0.07 to 0.87 with mean 0.44.

Therefore, we will report here full results based on the nine both-nights NREM parameters obtained from the full 48-hour recording. Although we found no significant differences between the first and second nights, in light of the contradictory data in the literature about the first-night effect, we also report the main results based on second-night data only.

Age and gender effects by two-way ANOVA

Table 1 and Fig. 2 summarize the effects of age and gender on the nine NREM parameters (duration, total and maximum parameters as derived from each of the R&K, SWP and SW% plots) from the both-nights manual data set (59 subjects).

Two-way ANOVA demonstrated a significant decrease in all parameters with increasing age (Table 2), with all p values <0.002. The Student-Newman-Keuls test showed that this effect was mainly based on the difference between the youngest group (26–35 years) and the other age groups. This is also clear from Fig. 2. The magnitude of the difference is about 1 SD.

The six R&K- and SWP-based parameters were significantly smaller in males than in females (Table 2), with all p values <0.02. The three SW%-based parameters did not show this gender effect; p values ranged from 0.19 to 0.76 (Table 2).

Two-way ANOVA of second-night manual data confirms the age effect, with p values of <0.01 for all nine NREM parameters. These data also confirm the gender effect on the six R&K- and SWP-based parameters, with all p values <0.005. They also showed no gender effect on the three SW%-based parameters; p values ranged from 0.34 to 0.74.

Two-way ANOVA of both-nights automatic data (74 subjects) confirms the age effect with p values of <0.006 for all NREM parameters. These data also confirm the gender effect on the six R&K- and SWP-based parameters, with all p values <0.015. They also showed no gender effect on the three SW%-based parameters; p values ranged from 0.31 to 0.99.

Interaction of age and gender effects

The three two-way ANOVAs described above detected weak interactions between age and gender in two parameters. For total based on SWP and for max-

TABLE 2. *ANOVA analysis (p values) of Age and Gender effects on the nine NREM parameters*

	Age	Gender	Age × Gender
Duration R&K	0.000	0.005	0.46
Duration SWP	0.000	0.000	0.67
Duration SW%	0.001	0.635	0.51
Total R&K	0.000	0.001	0.38
Total SWP	0.000	0.000	0.10
Total SW%	0.001	0.762	0.55
Maximum R&K	0.000	0.014	0.76
Maximum SWP	0.000	0.000	0.05
Maximum SW%	0.000	0.190	0.58

Note that both age and gender have highly significant effects on the six amplitude-dependent parameters (based on R&K or slow-wave power, SWP), whereas for the three amplitude-independent parameters (based on slow-wave continuity, SW%), age has a significant effect but gender does not.

imum based on SWP, age and gender interacted not quite significantly in the both-nights manual data set ($p = 0.10$ and 0.05) and in the second-night manual data set ($p = 0.06$ and 0.06), but they interacted significantly in the both-nights automatic data set ($p = 0.04$ and 0.01). Age and gender effects in these two parameters were therefore further assessed by one-way ANOVA on the both-nights manual data set.

The gender effect was confirmed for both parameters. In all age groups females were found to have higher values of both parameters than men in the same age group. This difference was significant ($p < 0.01$) in age groups 26–35 years and 66–75 years. The other two age groups had relatively large variance and few subjects (see Table 1).

The age effect was also confirmed for both parameters. In both gender groups, both parameters decreased with increasing age; the effect was significant ($p < 0.002$) for both males and females.

In the remaining seven parameters, age and gender did not interact in any of the data sets (all p values >0.25).

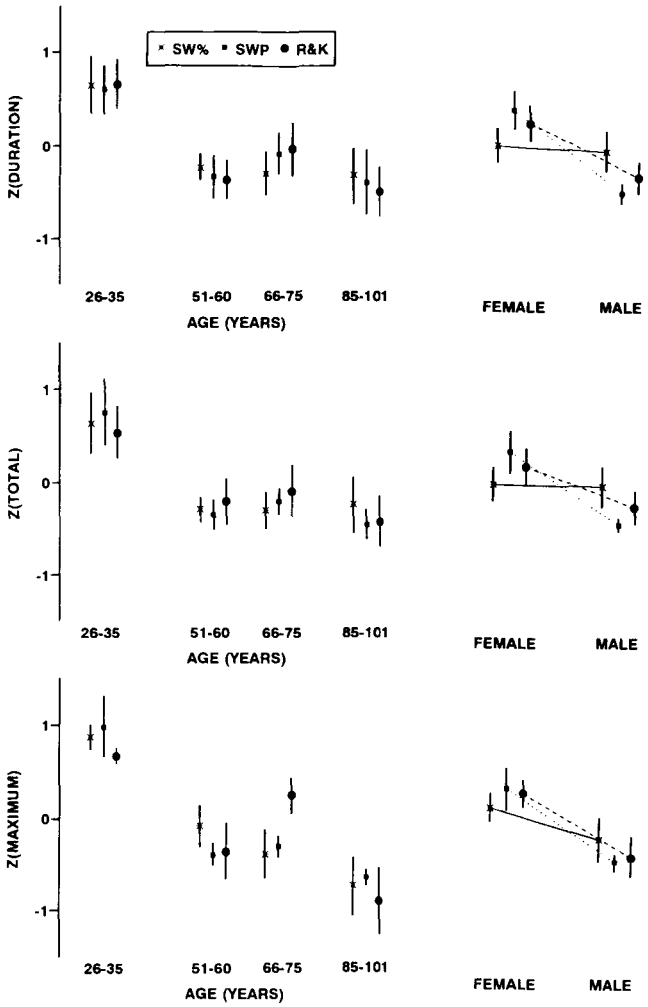

FIG. 2. Age and gender effects on, from top to bottom, NREM durations, totals and maxima. From left to right are the four age groups and both gender groups. Each NREM parameter was Z-transformed, thus normalizing its whole-group (all ages and both genders) mean and SD to 0 and 1, respectively. The vertical calibration indicates the difference (expressed in number of SDs) from the whole-group mean. The vertical bars show the means and the 95% confidence intervals of (from left bar to right bar in each cluster) the SW%-, SWP- and R&K-derived and Z-transformed parameters. Analyses are based on both nights, and include manual artifact rejection. Note that the age effect is similar in all nine parameters but the gender effect appears only in the parameters that are not based on SW%.

DISCUSSION

The SW%, as defined by its principle of computation, estimates which fraction (0–100%) of currently present slow-wave activity is continued in the near-future EEG. Therefore, direct amplification of EEG amplitudes does not influence SW%. However, modulation of EEG amplitudes through modulation of continuity (i.e. through inhibition of resonating neuronal feedback loops) does influence SW%. Therefore, factors that directly act on EEG amplitudes do affect SWP and R&K stages, but not SW%.

The computations of SWP and SW% involve manual and automatic artifact rejection. Still, in principle, remaining artifacts might depend on age or gender, and thus bias the results. We argue that this is not the case here. All SWP-based age and gender effects confirmed all R&K-based effects. In addition, the maximum parameters result from the epochs with the highest EEG amplitudes, and are therefore unlikely to be affected by artifacts. These maximum parameters were found to confirm all effects on durations and totals. Finally, all results from the automatic data set confirmed all results from the manual data set. We conclude that possible remaining artifacts are not responsible for the observed age and gender effects.

The present report confirms previous findings which

demonstrate that SWS decreases with age (5,21–30). The age effect from 30 to 55 years is substantial: it is about equal to interindividual differences (Table 1, Fig. 2).

The amplitude-independent parameters based on SW% assess the age effect with the same statistical power as the amplitude-dependent ones based on SWP and R&K. This suggests that age really affects the slow-wave resonating mechanism, and through this the EEG amplitudes. This effect could either be the result of actual loss of neural pathways (while model and model-based analysis still "think" that they are there), reduced activation of these pathways or both.

It is well known (5,21,30) that females have higher amplitudes of SWS EEG than males. In fact, females have, in general, higher EEG amplitudes than males (31–33). This is confirmed by our R&K- and SWP-based results (all p values <0.015). However, the amplitude-independent parameters (based on SW%) actually contradict a gender effect (all p values >0.15). Because of the age results described above, it is unlikely that the SW%-based parameters would be much less sensitive than the other methods. Therefore, it seems that gender has a direct effect on EEG amplitudes and does not affect the internal generation (i.e. resonance) of slow waves in the EEG.

This non-sleep-related gender effect on EEG amplitude might be caused by gender-related anatomic differences (5) such as head size (which also affects electrode positions), thickness of the skull, brain anatomic orientation, cell density and anatomy, electrochemical capacity of cells, etc. These variables would then bias the R&K- and SWP-based NREM sleep parameters. In our study this bias is substantial: the maximum SWP in females is about twice as high as in males (Table 1), which corresponds to about 40% higher amplitude maxima.

This bias is not accounted for in R&K scoring rules or in amplitude-dependent computerized analyses. Therefore, these methods could suggest that females sleep deeper than males even when they actually do not. The model-based SW% analyzer is to be considered in this case, since it does not directly depend on EEG amplitudes.

The maximum parameters are obtained from only one epoch, while the duration and total parameters are summations over many epochs. Nevertheless, the maximum parameters showed at least the same statistical powers for assessing the age effect. Therefore, aging may primarily limit the maximum SWS intensity a person can reach. Whether, and for how long, this intensity is actually reached would also depend on sleep pressure.

In the model, rhythmic power (P) and slow-wave continuity (p) are related as follows (see Appendix):

$$P = D/(1 - p),$$

where D is a constant factor. If indeed, as suggested by our results, age affects the maximum SW% while gender directly affects P, then these effects can be formulated as follows:

$$SWP_{max} = D(\text{gender})/[1 - SW\%_{max}(\text{age})],$$

where SWP_{max} is the maximum SWP of the EEG, D(gender) is a gender-dependent constant factor and $SW\%_{max}$(age) is the age-dependent maximum SW% that ranges from 0 to 1.

According to this model, gender and age effects on SWP_{max} multiply. This may explain why the ANOVA, which assumes addition of independent effects, can only explain the results by assuming interaction between age and gender. In fact, when applying logarithmic transformation to SWP_{max}, thus transforming multiplicative effects into additive ones, the ANOVA confirmed the main effects (age and gender, $p = 0.000$), but no longer detected such interaction ($p = 0.92$). This suggests that age and gender do not interact, and that their effects on maximum SWP multiply.

Acknowledgements: Huub Middelkoop advised M.S.M. about statistics. Ad Janssen made the data acquisition hardware and software. Gerard van de Giessen made the figures. Laurel Beecher corrected language and style in this article.

APPENDIX

The model-based analyzer

The model is a technical description of a general physiological principle behind the generation of slow waves and other rhythmic activity (7,15,16). The main idea is as follows.

Artificial versions of neuronal networks can produce realistic rhythms (7,8,15) while driven by noise. They do so because every cell is physically connected to many others; the interconnecting cells can form closed loops. These loops can carry activity from "under" the electrode to the future activity under that same electrode. In other words, the neuronal activity can cycle or echo through these loops, thus resonating rhythmical activity. Such loops can also be present within single cells. If the pathways involved are relatively slow (for instance because they are relatively long), the resonating rhythm will also be slow. Depending on the brain state (here sleep depth), a fraction (0–100%) of these potentially resonating loops is activated and actually resonates, resulting in the corresponding sleep-related slow-wave intensity.

This principle is kept in the simplified technical model (Fig. 3, upper part) first described by Kemp and Blom (14). Random noise (dw, representing incoming

activity, e.g. from membranes and external sources) drives the model. Internal activity (du, representing the average group activity of neuronal cells) cycles through the feedback loop (the resonance filter G, representing the potentially resonating closed loops). L is lowpass volume conduction. The feedback gain (p, representing activation or de-inhibition of resonating loops) determines the strength of the resonating rhythmic component. In this model, p ranges from 0% (no rhythms) to 100% (infinitely large rhythms). The relationship between p and the resulting mean rhythmic power, P, is: $P = D/(1 - p)$, where D is a constant factor.

Depending on the selected value of p, the model generates realistic simulations of EEG with K complexes and slow-wave activity (Fig. 3, lower part) (8,13). A striking feature of the simulations is that rhythms realistically wax and wane (14), even with constant p and constant model parameters. This is due to the fact that the rhythms are randomly either reinforced (waxing) or attenuated (waning) by the input noise.

According to the model, the functional state that relates sleep depth to the generation of SWS-EEG is the feedback gain, p. It reflects how many of the potentially resonating closed loops are actually activated.

This has a very important implication for analysis. The feedback filter, G, of the model describes the potential continuation of current low-frequency EEG in the future signal. This potential future rhythmic component, s, can be predicted (usually we predict 20 milliseconds or 10 milliseconds ahead) simply by passing the recorded EEG through the feedback filter. The actual future rhythm can be smaller if the feedback gain (i.e. actual activation of potentially resonating loops, p) is less than 100%. In this case, part of the potentially available resonating pathways are inhibited. In fact, p equals the extent (0–100%) to which the potential rhythm, s, actually shows in the future signal, du, i.e. the extent (0–100%) to which the slow-wave component is continued into the future. This continuity is maximum-likelihood-estimated as follows (11,12): $SW\% = (s \cdot du)/(s^2 \cdot dt)$. One can check this by substituting the model equation: $du = p \cdot s \cdot dt + dw$.

The model offers an interesting method for artifact rejection because the model predicts that, on average and for any p, the following expression is true: $(s^2 \cdot dt) - (s \cdot du) - \pi \cdot B = 0$, where B is the bandwidth (in Hz) of the feedback filter G. Artifacts are not predicted by the model and in many cases appear to make this expression not true. In particular, applying high and low thresholds to the expression provides relatively good detection of high-frequency and low-frequency artifacts, respectively.

The model-based analysis performed much better than power-based (e.g. Fourier) analyses in alpha blocking experiments (18). It also appears to be less sensitive to artifacts such as EMG, EOG or body movements (19), probably because the analysis is tuned to an EEG-generating mechanism.

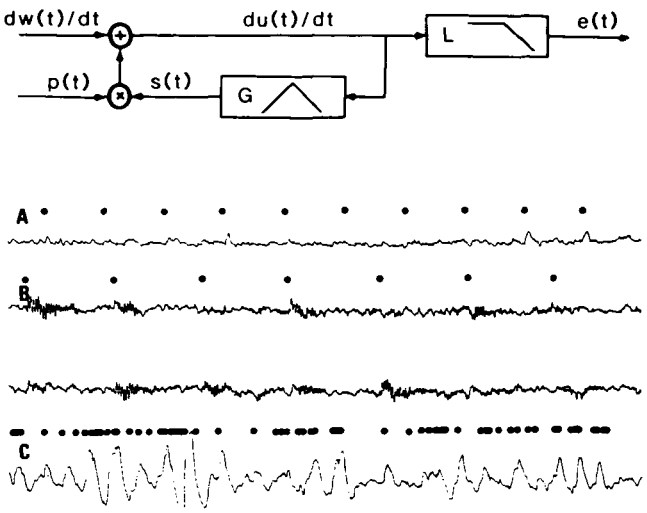

FIG. 3. Upper part: block diagram of EEG, e(t), generator model with activated percentage, p(t), of potentially resonating pathways, G. The model is driven by random noise (dw/dt), and contains a volume conductor compartment, L. Lower part: EEG simulations by the model, with pulse events (heavy dots) added to the input noise. See Caekebeke et al. (8) for details. From top to bottom: A. constant G and p, tuned to R&K stages 0–1. B. constant G and p, tuned to R&K stage 2. C. constant G and p, tuned to R&K stages 3–4. In simulations A and B, the pulse events are periodic. In simulation C, the pulse events are random.

In general, the model and the model-based slow-wave continuity, SW%, offer a direct physiological and functional interpretation. For example, the model simulations demonstrated that waxing and waning can occur while slow-wave resonance (sleep depth?) is constant. Also, SW% equals the percentage of the potentially available resonating pathways that is not inhibited, i.e. that is active.

REFERENCES

1. Rechtschaffen AA, Kales A, eds. *A manual of standardized terminology, techniques and scoring system for sleep stages of human subjects.* Washington, DC: Public Health Service, U.S. Government Printing Office, 1968.
2. Achermann P, Borbely AA. Dynamics of EEG slow wave activity during physiological sleep and after administration of benzodiazepine hypnotics. *Hum Neurobiol* 1987;6:203–10.
3. Allen SR, Seiler WO, Stahelin HB, Spiegel R. Seventy-two hour polygraphic and behavioral recordings of wakefulness and sleep in a hospital geriatric unit: comparison between demented and nondemented patients. *Sleep* 1987;10:143–59.
4. Carskadon MA, Dement WC. Normal human sleep: an overview. In: Kryger M, Roth T, Dement WC, eds. *Principles and practice of sleep medicine.* WB Saunders Company, 1989:3–13.
5. Dijk DJ, Beersma DGM, Bloem GM. Sex differences in the sleep EEG of young adults: visual scoring and spectral analysis. *Sleep* 1989;12:500–7.
6. Kemp B. A proposal for computer-based sleep/wake analysis. *J Sleep Res* 1993;2:179–85.

7. Lopes da Silva FH, Van Rotterdam A, Barts P, Van Heusden E, Burr W. Models of neuronal populations: the basic mechanisms of rhythmicity. *Prog Brain Res* 1976;45:281–308.
8. Caekebeke JFV, Van Dijk JG, Rosa AC, Kemp B. A model relating K-complexes to spontaneous slow-wave activity during sleep. In: Terzano MG, Halasz PL, Declerck AC, eds. *Phasic events and dynamic organization of sleep.* New York: Raven Press, 1991:41–51.
9. Armitage R, Roffwarg H. Distribution of period-analyzed delta-activity during sleep. *Sleep* 1992;15:556–61.
10. Feinberg I, March JD, Fein G, Floyd TC, Walker JM, Price L. Period and amplitude analysis of 0.5–3 c/sec activity in NREM sleep of young adults. *Electroencephalogr Clin Neurophysiol* 1978; 44:202–13.
11. Kemp B. Model-based monitoring of human sleep stages. Thesis. Twente University, Enschede, 1987:60–95.
12. Kemp B, Lopes da Silva FH. Model-based analysis of neurophysiological signals. In: Weitkunat R, ed. *Digital biosignal processing.* Amsterdam: Elsevier Science Publishers, 1991:129–55.
13. Kemp B. Cerebral information processing estimated by unpredictability of the EEG. *Clin Neurol Neurosurg* 1992;Suppl 94: S103–5.
14. Kemp B, Blom HAP. Optimal detection of the alpha state in a model of the human electroencephalogram. *Electroencephalogr Clin Neurophysiol* 1981;52:222–5.
15. Lopes da Silva FH, Hoeks A, Smits H, Zetterberg LH. Model of brain rhythmic activity: the alpha rhythm of the thalamus. *Kybernetik* 1974;15:27–37.
16. Steriade M. Basic mechanisms of sleep generation. *Neurology* 1992;42, Suppl 6:9–17.
17. Kamphuisen HAC, Kemp B, Kramer CGS, Duijvestijn J, Ras L, Steens J. Long-term sleep deprivation as a game. *Clin Neurol Neurosurg* 1992;Suppl 94:S96–9.
18. Kemp B. Accurate measurement of flash-evoked alpha attenuation. *Electroencephalogr Clin Neurophysiol* 1983;56:248–53.
19. Kemp B, Värri A, Da Rosa A, Nielsen KD, Gade J, Penzel T. Analysis of brain synchronization based on noise driven feedback models. *Proc IEEE-EMBS* 1991;13:2305.
20. Kemp B, Kamphuisen HAC. Model-based sleep analysis. In: Peter JH, Penzel T, Podzus T, Von Wichert P, eds. *Sleep and health risk.* Berlin: Springer-Verlag, 1991:50–7.
21. Wauquier A, Van Sweden B, Lagaay AM, Kemp B, Kamphuisen HAC. Ambulatory monitoring of sleep–wakefulness patterns in healthy elderly males and females (>88 years): the "senieur" protocol. *Am Geriatr Soc* 1992;40:109–14.
22. Ehlers CL, Kupfer DJ. Effects of age on delta and REM sleep parameters. *Electroencephalogr Clin Neurophysiol* 1989;72:118–25.
23. Feinberg I. Changes in sleep cycle patterns with age. *J Psychiatr Res* 1974;10:283–306.
24. Feinberg I, Koresko RL, Helter N. EEG sleep patterns as a function of normal and pathological aging in man. *J Psychiatr Res* 1967;5:107–44.
25. Feinberg I, March JD, Floyd TC, Fein G, Aminoff MJ. Log amplitude is a linear function of log frequency in NREM sleep EEG of young and elderly normal subjects. *Electroencephalogr Clin Neurophysiol* 1984;58:158–60.
26. Feinberg I. Effects of maturation and aging on slow-wave sleep in man: implications for neurobiology. In: Wauquier A, Dugovich C, Radulovacki M, eds. *Slow wave sleep: physiological, pathophysiological and functional aspects.* New York: Raven Press, 1989:31–47.
27. Hayashi Y, Endo S. All-night sleep polygraphic recordings of healthy aged persons: REM and slow-wave sleep. *Sleep* 1982; 5:277–83.
28. Kahn E, Fisher C. The sleep characteristics of the normal aged male. *J Nerv Ment Dis* 1969;148:477–94.
29. Reynolds CF, Monk TH, Hoch CC, et al. Electroencephalographic sleep in the healthy "old": a comparison with the "young old" in visually scored and automated measures. *J Gerontol Med Sci* 1991;46:M39–46.
30. Webb WB. Sleep in older persons: sleep structures of 50- to 60-year-old women. *J Gerontol* 1982;37:581–6.
31. Bliwise DL. Sleep in normal aging and dementia. *Sleep* 1993; 16:40–81.
32. Veldhuizen RJ, Jonkman EJ, Poortvliet DCJ. Sex differences in age regression parameters of healthy adults—normative data and practical implications. *Electroencephalogr Clin Neurophysiol* 1993;86:377–84.
33. Duffy FH, Albert MS, McAnuty G, Garvey AJ. Age-related differences in brain electrical activity of healthy subjects. *Ann Neurol* 1984;16:430–8.